

Review

Materials and Processing of Lithium-Ion Battery Cathodes

Wenbin Fu ^{1,*}, Yice Wang ², Kanglin Kong ³, Doyoub Kim ¹, Fujia Wang ¹ and Gleb Yushin ^{1,*}¹ School of Materials Science and Engineering, Georgia Institute of Technology, Atlanta, GA 30332, USA² School of Chemistry and Biochemistry, Georgia Institute of Technology, Atlanta, GA 30332, USA³ George W. Woodruff School of Mechanical Engineering, Georgia Institute of Technology, Atlanta, GA 30332, USA

* Correspondence: wenbin.fu@mse.gatech.edu (W.F.); yushin@gatech.edu (G.Y.)

Abstract: Lithium-ion batteries (LIBs) dominate the market of rechargeable power sources. To meet the increasing market demands, technology updates focus on advanced battery materials, especially cathodes, the most important component in LIBs. In this review, we provide an overview of the development of materials and processing technologies for cathodes from both academic and industrial perspectives. We briefly compared the fundamentals of cathode materials based on intercalation and conversion chemistries. We then discussed the processing of cathodes, with specific focuses on the mechanisms of a drying process and the role of the binders. Several key parameters for the development of thick electrodes were critically assessed, which may offer insights into the design of next-generation batteries.

Keywords: lithium-ion batteries; cathodes; electrode processing; electrode design

1. Introduction

The challenge of climate change is pushing countries all around the world to realize an energy transition from traditional fossil fuels to clean energy resources [1,2]. To realize this transition, various energy storage systems were developed in recent decades. Among them, a lithium (Li)-ion battery (LIB) is one of the most successful systems and it promoted the revolution of electronics, wearables, transportation, and grid energy storage [3–5]. With the development of electric transportation from road to sea and air (Figure 1a), the future will clearly be electric. This transition is not only driven by the progress in energy- and electronic-related technologies, but also by the rapidly falling prices of LIBs [6,7]. In 1991, the cell price of LIBs was high as ca. 5000 \$ kWh⁻¹, but in 2020, it was 101 \$ kWh⁻¹, as shown in Figure 1b [7]. As predicted by us, the price of LIBs will continue falling all the way to ca. 30–40 \$/kWh by around 2040–2050 [8], which, in addition to expected cycle stability gains, is expected to provide more opportunities for the development of LIBs towards broader potential applications.



Citation: Fu, W.; Wang, Y.; Kong, K.; Kim, D.; Wang, F.; Yushin, G. Materials and Processing of Lithium-Ion Battery Cathodes. *Nanoenergy Adv.* **2023**, *3*, 138–154. <https://doi.org/10.3390/nanoenergyadv3020008>

Academic Editors: Kwang-Sun Ryu and Ya Yang

Received: 24 March 2023

Revised: 3 May 2023

Accepted: 12 May 2023

Published: 19 May 2023



Copyright: © 2023 by the authors. Licensee MDPI, Basel, Switzerland. This article is an open access article distributed under the terms and conditions of the Creative Commons Attribution (CC BY) license (<https://creativecommons.org/licenses/by/4.0/>).

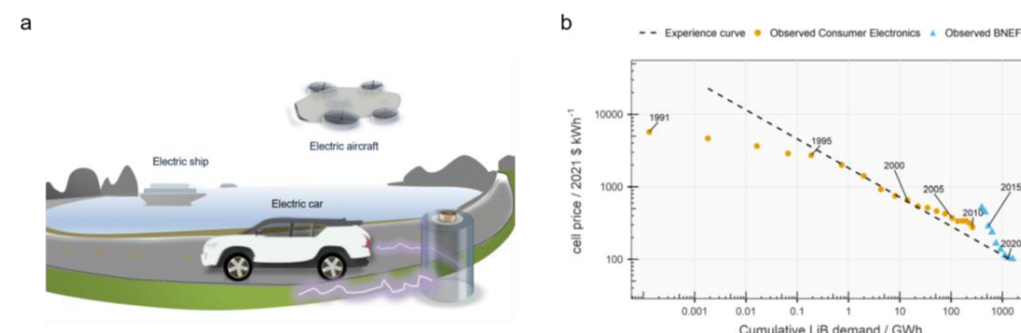


Figure 1. (a) An illustration of future electric transportation. (b) Observed cell prices from 1991 to 2021. (b) was reproduced from Ref. [7] (the observed BNEF data were from BloombergNEF).

A LIB cell mainly consists of two electrolyte-filled electrodes (cathode and anode), a porous separator membrane also filled with the same liquid electrolyte, and a sealing case. Among these components, the cathode usually has the highest weight fraction and often plays a dominant role in attainable cost and many cell performance characteristics, especially those that are related to battery weight, safety, and calendar life. Conventional intercalation cathodes such as lithium iron phosphate (LiFePO_4 , LFP), lithium cobalt oxide (LiCoO_2 , LCO), lithium manganese oxide (LiMn_2O_4 , LMO), and lithium nickel cobalt manganese (or aluminum) oxide (NCM or NCA) are widely used in current LIBs [9]. However, the relatively low energy density and specific energy of these materials could be a barrier for some applications. Additionally, the increasing prices, the limited resources, various challenges with environmentally friendly mining and the toxicity of nickel (Ni) and cobalt (Co) minerals bring additional challenges for large-scale applications. Conversion-type cathodes such as sulfur (S), metal (e.g., iron, Fe) fluorides (FeF_3 , FeF_2), and oxyfluorides could be alternatives because of their higher specific energy and lower cost [10–12]. In the past two decades, great efforts were devoted to different cathode materials. However, both conventional and much more so conversion-type cathodes still suffer from various issues [10]. In addition to cathode materials themselves, improvements in electrode processing technologies are also crucial to cell performance and cost [13–15]. The development of advanced processing technologies calls for critical considerations of the fabrication procedures, such as mixing, drying, pressing, and lamination [13]. Additionally, the use of advanced binder systems is important for the fabrication of high-performance cathodes, with considerable impacts on their mechanical and electrochemical properties. To design of a cathode electrode with optimal performance, basic parameters such as the defects and crystallinity of cathode particles, particle size and distribution, electrode architecture, and porosity and tortuosity should be taken into consideration [16–18].

This review aims to provide a comprehensive overview of materials and processing technologies currently utilized in LIB cathodes. We discuss the main features and issues of cathode materials of both intercalation and conversion types. We then delve into the processing technologies and binder systems for cathode electrodes, and analyze the key parameters that determine the electrodes' performance. The discussion also covers the mechanical properties of cathodes from particle to electrode levels. We present these discussions from both academic and industrial perspectives, which will enable students, researchers, engineers, and others to gain a thorough understanding of the fundamentals involved in LIB cathodes.

2. Cathode Materials

Current LIBs are mainly built on intercalation chemistry, which enables the intercalation/extraction of Li ions in/from bulk electrode materials for thousands of cycles. Conventional intercalation cathodes mainly include LFP, LCO, LMO, NCM, and NCA. Among them, LCO, LFP, and NCM were particularly widely used in the battery market for electronics (mostly LCO) and electric vehicle (EVs) (mostly LFP, NCM and NCA). However, these materials are still limited by the attainable energy density, specific energy, and cost. Conversion cathode materials could be the solution, considering that conversion-type anodes (e.g., silicon (Si)) were successfully commercialized in recent years and their production and market penetration are growing rapidly. The replacement of conventional cathodes by conversion-type cathodes, such as sulfur, metal fluorides, and oxyfluorides can largely increase the specific energy and reduce the cost of the LIB cells. However, there are still significant limitations needed to be overcome before the scale-up and broad adoption of conversion-type cathodes takes place. Figure 2 illustrates the crystal structures of typical intercalation and conversion cathode materials.

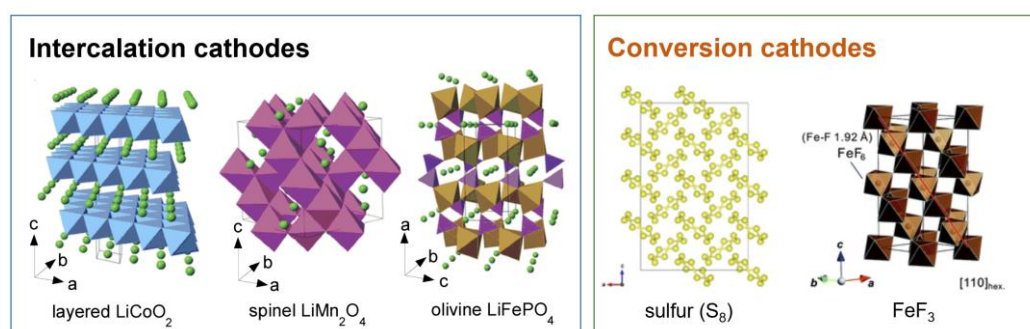


Figure 2. Crystal structures of typical intercalation cathodes and conversion cathodes. Figures adapted with permission from Ref. [19] MDPI, Ref. [20] Elsevier, and Ref. [21] RSC.

2.1. Intercalation Cathodes

Currently, intercalation cathodes are widely used in LIBs due to their high potentials (versus Li/Li^+), long cycle life, and good structural stability in air. Layered LCO, spinel LMO, and olive LFP were widely studied in the past few decades. The first-generation commercial LIBs were built on LCO in 1990s. However, the limited energy density and high cost of Co are the major issues that hinder their further applications. In addition, there are major issues with Co supply chain [22,23]. The use of LFP or LMO could overcome supply chain limitations and reduce the cost of cathode materials, but cell energy would be reduced as well. In addition, LFP (and to a lesser extent LMO) cathodes are not economical to recycle [24]. Yet, in many cases, cost, supply chain and safety are still the major concerns. As such, LFP was recently more and more used in EV batteries despite its low energy density. Ni-based layered transition metal oxides such as NCM and NCA could provide higher energy density than LFP and LMO, but cost less than LCO, which enables them to be used in state-of-the-art EVs with a longer driving range. In recent years, researchers explored ultrahigh-Ni layered NCM/NCA, Li- and/or Mn-rich NCM, and phosphate polyanion cathodes and pushed their energy density and cycle stability to satisfy the requirements for practical applications [25–27]. In general, intercalation cathodes could undergo a capacity degradation due to surface phase transition, the dissolution of transition metals, gas release, or microcracking [12,28,29]. To address these challenges, researchers proposed various strategies, including the use of single crystalline materials (which do not crack), doping, protective surface layer formation, and advancing applications of electrolyte additives that better passivate the cathode surface, among others [12]. For example, using single-crystal $\text{LiNi}_{0.6}\text{Co}_{0.2}\text{Mn}_{0.2}\text{O}_2$ (NCM622) for LIB pouch cells can achieve significantly better cycle performance with a capacity retention of 83% after 3000 cycles, compared to polycrystalline NCM622 [30]. The introduction of various dopants, such as 1 mol.% molybdenum (Mo), for example, to Ni-rich layered oxide cathodes enabled a higher voltage and higher energy density, such as 880 Wh kg^{-1} cathode for 1000 stable cycles in layered Co-free NCM901 [31]. Despite these advances, it may be difficult to further improve their energy density of these materials by a significant degree, considering the theoretical limitations from intercalation chemistry.

2.2. Conversion Cathodes

As alternatives to current intercalation cathodes, conversion-type cathodes featuring sulfur (S) and metal fluorides can make use of conversion reactions during charging/discharging and achieve multiple electron transfers, which enables higher specific capacity and energy to be attained. Figure 3 compares the specific energy for a cell using different cathodes coupled with a conventional graphite (C) anode (Figure 3a), next-generation Si anode (Figure 3b), or Li metal anode (Figure 3c). Compared to conventional intercalation cathodes, the conversion-type cathodes such as Li_2S , CuF_2 , and FeF_3 higher specific energies, especially when coupled with Si (Figure 3b) or Li metal anodes (Figure 3c), such as Li_2S -Si, CuF_2 -Si, Li_2S -Li, and CuF_2 -Li systems. In previous reviews, researchers critically discussed the pros and cons of different conversion cathodes [10,32,33].

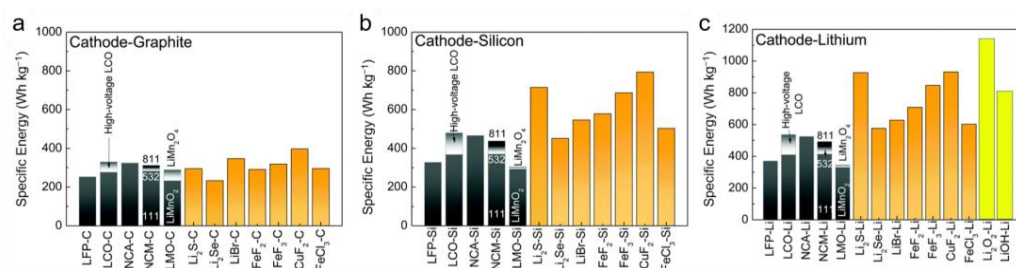


Figure 3. Specific energies of Li-ion batteries using intercalation or conversion cathodes coupled with (a) graphite (C), (b) Si or (c) Li metal anodes. Figures adapted with permission from Ref. [10], RSC. The specific energies were estimated based on the unit stacks in Li batteries detailed in Ref. [10].

Despite their high energy densities, conversion cathodes currently suffer from a much faster capacity degradation during cycling compared to intercalation cathodes. In many cases, conversion cathodes can be only charged/discharged for few hundreds of cycles or less, especially in high areal capacity loadings or at elevated temperatures. The decreased cycle stability could be attributed to several issues, such as the dissolution of active species, the large structural changes, and side reactions [12]. For example, in a Li-S cell, the dissolution of polysulfide intermediates could result in a shuttle effect, which seriously affect the cell performance [34]. Additionally, the lack of stable interphase on cathodes could also limit their electrochemical stability, in contrast to a SEI layer formed on anodes during first few cycles [35–37]. As such, the stabilization of cathodes and interphases is essentially important to the development of next-generation LIBs. Effective strategies could cover the development of cathode coatings, the addition of advanced electrolytes or additives, the functionalization of separators/interlayers, or the use of multifunctional binders. We critically discussed these strategies in an article [12].

3. Electrode Processing

Conventionally, the manufacturing of cathode electrodes is based on a slurry-based process, which starts from mixing active and inactive materials (binders, conductive additives) with a suitable solvent to form a uniform slurry, then coating the slurry onto a current collector (Al for cathodes) foil and drying, then calendaring (densifying) the electrode to attain high packing density and high volumetric capacity, then electrode cutting suitable shapes, assembling the electrodes and membranes into a cell, and then finally conducting a formation cycle (initial charge and discharge, often at elevated temperatures to accelerate the process), degassing and testing for capacity retention and quality, as shown in Figure 4 [38]. In a slurry-based process, the drying process (removing a slurry solvent) is the key that often defines electrode behavior and a significant factor to total electrode fabrication costs. The drying step often involves multiple transport mechanisms (such as diffusion, convection, and migration) and is dependent on the involved volumetric sources/sinks (such as phase change, chemical bonding, gravity) and driving forces (such as local temperature, concentration, and pressure) [39]. In the following subsections, we mainly discuss the conventional slurry-based process, the role of the polymer binders, and the recently introduced solvent-free dry electrode process.

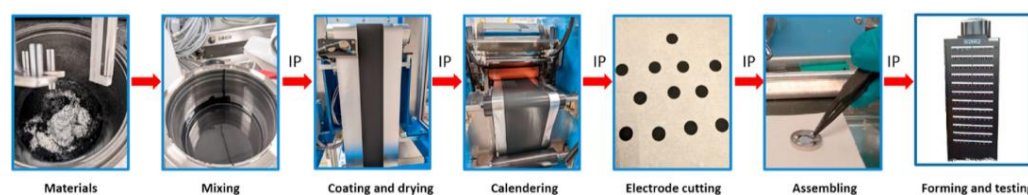


Figure 4. A schematic flow to manufacture battery electrodes. (IP, intermediate product). Figure panel adapted with permission from Ref. [38], Elsevier.

3.1. Drying Process

In the slurry-based process, the drying process is one of the complicated and decisive procedures, which influences the porous structure formation and the distribution of cathode particles, binders, and conductive additives in the electrodes. A typical drying process can be typically classified to two stages, including surface solvent evaporation and pore-emptying evaporation [40]. As shown in Figure 5, the surface solvent evaporation is a dominant and fast solvent removal process [41], which could enable over the removal of 90% solvent with a half of time period in the total drying process [42].

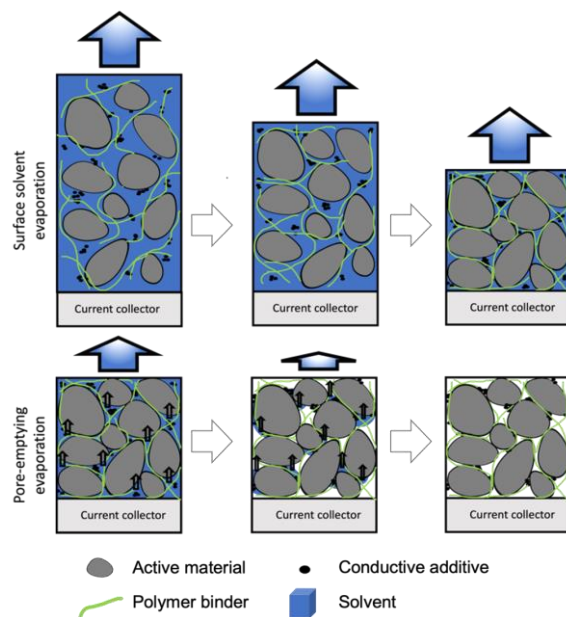


Figure 5. Schematics of drying process including surface solvent evaporation and pore-emptying evaporation stages. The blue arrow symbolizes solvent evaporation.

In the beginning, the solution is dilute and different components suspend in slurry, resulting a sufficiently large and constant temperature enclosure. In ambient environment, the partial pressure of the solvent remains constant and contributes to constant evaporation rate [43]. Most of the solvent evaporation happens from the liquid surface of the solid-solvent slurry and the film shrinkage further processes until the active material consolidation finishes. Through a gravity force and due to a high evaporation rate, heavy active material particles approach each other and finally sediment to form a compact active material skeleton with tiny pores, in a process called film consolidation [41], where the thickness of consolidated film then remain fixed through the remaining solvent evaporation. In this case, the relatively light mass of conductive additives (e.g., carbon black) make it barely influenced by gravity and so the additives typically remain relatively uniformly distributed in slurry through the solvent diffusion.

In the second stage, the pore-emptying evaporation, the remaining solvent residue inside the pores is fully evaporated, finally forming a completely dry electrode coating on the current collector. However, because the evaporation rate significantly drops from previous constant evaporation rate to a much lower number, the removal of last 10 percent of solvent could take nearly the same time as the removal of first 90 percent of the solvent in the first stage [42,43]. The mechanism of the pore-emptying evaporation is more complex. In this case, the consolidation of active materials, the thickness of the coating, the dimensions, and the porous structure of coating are already fixed. The microstructure of the coating is only tweaked by the re-distribution of conductive additives and the binder polymer. Subject to a settled porous structure made by the backbone of active material, the evaporation triggered diffusion often induces slight (local) movement of the binder mixed with conductive additive and smaller active material particles and typically deposit them

at narrow pathways between bulky (largest) active material particles. The long-distance migration of binder and conductive additives are no longer available due to a relatively small evaporation rate and greatly increased friction forces.

3.2. The Role of Binder

Despite being an inactive component and occupying a small portion of the electrodes, the polymer binder typically plays a vital role in the electrode fabrication and performance. In conventional electrode design, the selection of a binder and its solvent could determine the required fabrication procedures. Overall, polymer binders make use of physical or chemical bonding interactions to build a porous and mechanically stable structure for electrodes, which need to withstand various stresses involved in battery fabrication and charging and discharging cycling [44–46]. The binder also helps to support the uniform dispersion of active materials. It is crucial to understand the adhesion mechanisms of binders to optimize its performance in various cell form factors and designs. In general, the adhesion mechanisms could cover macroscopic theory and molecular level theory. In both theories, the pre-binding procedure are similar. In a slurry stirring (or a dry powder blending), the polymer binder particles experience dissolution, diffusion, and penetration contacting with active materials and conductive additives (typically carbon black, CB) [47]. The binding process, “hardening”, is commonly triggered by diverse physical reaction mechanisms (such as the solvent evaporation after electrode casting or the cooling process after melting binder in dry electrode process) causing actual physical or inter-molecular adhesion between various particles and the current collector [47]. In a macroscopic theory, the mechanical interlocking, electrostatic force is accounted to strong adhesion force between two objects, which are ubiquitous in our daily life. The molecular level theory of binding mechanism could be more intricate and difficult to observe, but more convincing for scientists. For example, the chemical intermolecular interaction (such as the hydrogen bonding and Van der Waals forces), the interdiffusion of polymer chain, the chemical adsorption all occur on a molecular level [48,49]. Nevertheless, the chemical intramolecular interaction (such as the covalent bonding, the metallic bonding, and the ionic bonding) between the binder and the particles are exceptional. An integration of a whole electrode system only within the scope of the intramolecular level interactions may be unrealistic, but it, nonetheless, inspires researchers to search novel-electrode designs.

Today, polyvinylidene fluoride (PVDF) is widely used as a binder in LIB electrodes due to its strong binding via a Van der Waals force and large commercial production. However, to prepare cathode slurry, some organic solvents, typically featuring toxic and expensive N-Methyl-2-pyrrolidone (NMP) must be used. The use of the PVDF/NMP binder system suffers from several drawbacks, including the poor electrical/ionic conductivity of the formed electrodes, costly drying process, the evaporation of toxic solvent, degradable structure, poor mechanical properties (especially when swollen in a binder), and weak protection for active material under high temperature or high voltage [50]. In recent years, researchers extensively explored novel binder systems to overcome those issues. Table 1 presents selected representatives of these binders and the cycle performance of their-based cathodes. Mixing PVDF with other NMP-tolerable polymers was explored to improve the dispersion of slurry components [51–54]. Recently, Yoo et al. reported a novel organosilicon binder which does not suffer from binder self-aggregation, which can reduce electrode tortuosity and enhance the electrode integrity by forming a binder web with both covalent and hydrogen bonding [55]. At a reasonably high mass loading (~8 mg/cm²; approximately half of commercial loadings), the prepared LCO electrodes can retain around 92% capacity after 100 cycles, which is insufficient for commercial applications, but promising, nonetheless.

Table 1. Selected binder systems for cathodes and their cycle performance in Li-ion cells.

Binder	Solvent	Cathode	Cycle Number	Retention	Ref.
PVDF	NMP	NCM ₁₁₁	200 @0.5C	86.3%	[56]
PVDF-HFP	NMP	NCM ₅₂₃	330 @1C	50%	[51]
Organosilicon binder	NMP	LCO	100 @0.5C	92%	[55]
PMMA	NMP	LFP	120 @1C	86.3%	[57]
(Hex:OE)PProDOTs	NMP	NCA	200 @C	87.9%	[58]
Fluorinated Polyimide	NMP	NCM	100 @0.2C	89%	[59]
PVDF-PS	NMP	NCM ₅₃₂	400 @1C	90%	[52]
Cellulose nanofibers	water	LFP	150 @2mA cm ⁻²	90%	[48]
P(MVE-LMA)	water	LNMO	400 @1C	92%	[60]
Lignin	alkaline water	LNMO	1000 @1C	94.1%	[61]
Alginate	water	LMO	120 @1C	97.7%	[62]
Pullulan	water	NCM ₅₂₃	500 @0.33C, 1C	83.33%	[63]
Guar gum	water	LNMO	250 @20 mA g ⁻¹	95.2%	[64]
Li-PAA	water	LVP	300 @1C	97.4%	[65]
Sodium alginate	water	CuF ₂	50 @0.05C	68.23%	[66]
rGO-Chitosan	aqueous acetic acid (1.5%)	S	1000 @1C	84%	[67]
CMC/acrylic emulsion	water/isopropyl alcohol	NCM ₅₂₃	100 @0.33C	97.3%	[68]

Aqueous solvent-based binders recently gained particularly strong interest, as using water in slurries can reduce the cost for electrode manufacturing and recycling, and additionally enable formation of a more homogenous slurry with active materials. Unfortunately, aqueous solvent-based binders typically also initiate new challenges, such as the dissolution of lithium and transitional metal ions from active materials in contact with water [69], corrosion of the Al current collector, cracking during electrode handling and drying (as aqueous binders may be more brittle), bubble formation, and delamination due to rapid solvent evaporation and significant binder shrinkage upon electrode drying [70–72]. Some possible solutions were suggested to address these challenges during aqueous processing, such as adding a buffer solution to mitigate a high pH at the slurry, using a carbon coated current collector, and controlling the solvent evaporation condition, among others [73]. The most common aqueous solvent-based binders are biomass polymer, which means their structures are more designable through chemical reaction to serve their multifunctional nature. Most recent studies on biomass-based binders such as cellulose nanofibers [48], lignin [61], guar gum [64], chitosan [67], carboxymethyl cellulose (CMC)/acrylic emulsion polymer [68] are listed in Table 1.

Binders not only provide a compact skeleton for active material but also can enhance electrochemical performance by mitigating some unpleasant side reaction in electrochemical reaction. In conversion cathodes (such as S, Se, metal sulfides, and fluorides), such approaches attracted increasing attention [12]. Yet, as previously mentioned, the successful utilization of conversion cathode in industrialization is hindered by multiple existing challenges, such as the shuttle effect by dissolution of lithium polysulfide, the blockage of conversion reactions by side products, among others [10]. Novel functional binders may be able to overcome those discussed drawbacks of conversion cathodes, as was demonstrated in the case of sodium alginate [66] and chitosan [67].

3.3. Dry Electrode Process

The PVDF/NMP binder system is not only expensive for high volume manufacturing but is also environmentally harmful. Although studies showed that water-based binder systems may potentially replace PVDF/NMP, they only became successfully commercialized for anode materials [47,49,74,75]. Their use still remains challenging for cathodes, because of the current collector corrosion, active particle deterioration, gas formation at elevated temperatures and voltages, and cracking of the electrodes (mostly thick electrodes) during drying process, to name a few [72,76]. In addition to the conventional slurry-based process, processing electrode through a solvent-free dry method may become very lucrative [77], because it can skip multiple costly procedures in battery manufacturing, such as the slow and expensive solvent evaporation [78–80]. As illustrated in Figure 6, the dry process enables a “powder-binder” electrode manufacturing to avoid the use of NMP or other solvents. In some designs, the dry process may begin with mixing and either dry spraying of active material, binder, and conductive additive onto a current collector [80], which allows binder particles and conductive particles to be decorating the surface of active material without causing significant agglomerates. The hot-roller pressing process is applied to melt the binder particles and allows the binder to wet the surface of active material and agglomerate with conductive additives [78,80]. The voids between active materials are partially filled with conductive framework of the melted binder mixed with conductive additives. Other investigated methodologies such as extrusion and 3D printing (with hot pressing) could also work for dry processing of electrodes [77,81,82], although agglomerates of hard cathode particles may induce excessive wear and tear to extrusion equipment and, thus, should be avoided at all costs. As well as fabrication of conventional LIBs, recent studies indicate that dry electrode process have great potential for the manufacturing of all-solid-state batteries (ASSBs) [83–87].

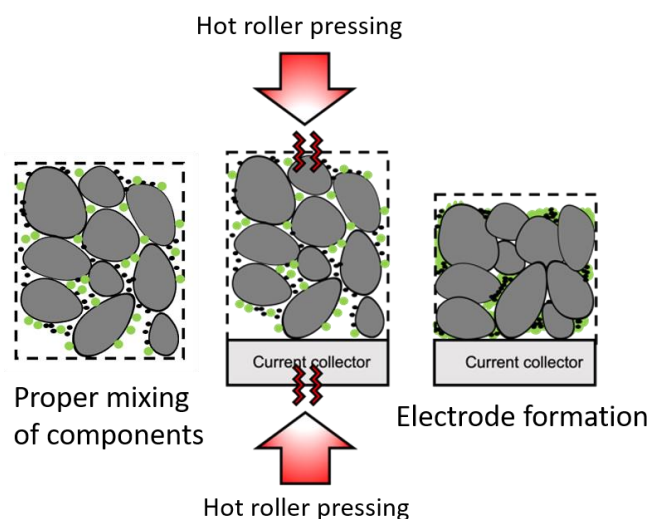


Figure 6. Schematics of dry electrode process.

4. Key Parameters for Cathode Electrodes

Increasing the thickness of cathode electrodes is a promising way to enhance pack energy. However, today, the design of thick electrodes over 80 μm is still challenging. This is because thicker and denser electrodes may slow down ion transport, reduce the utilization of battery materials, limit electrolyte infiltration and lower electrochemical performance, particularly rate capability [88–91]. Dense structures with highly compressed electrodes, thick coatings, and high concentrations of small particles can limit ionic conductivity due to the high tortuosity of pore networks and longer ion diffusion pathways [92–96]. Using thick electrodes can also lead to larger Li^+ concentration gradients, increasing resistance and reducing performance. To achieve optimal performance in energy/power densities, thick-

ness, and loadings, it is desirable to consider some key parameters (Figure 7), including the defect and crystallinity, particle size and distribution, tortuosity, and electrode architecture.

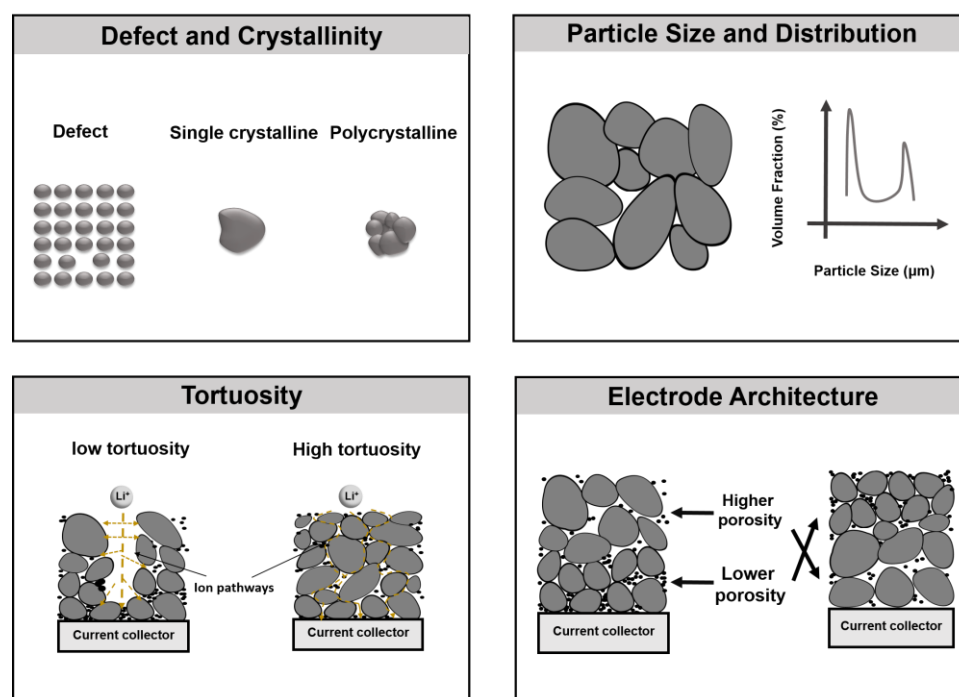


Figure 7. Key parameters for cathode electrodes, including defect and crystallinity, particle size and distribution, tortuosity and electrode architecture.

4.1. Defect and Crystallinity

Crystallographic defects, such as vacancies, interstitials, dislocations, grain boundaries, and others, widely exist in cathode crystals and could seriously affect the physical and (electro)chemistry performance of the cathodes [97]. Usually, these defects could result in accelerated structural and electrochemical degradations. Conventional cathodes such as NCM are composed of nanoparticles-aggregated secondary microspheres, which are known to suffer from fast capacity degradation and thermal instability due to the fast dissolution of grain boundary regions (the internal surfaces between the nanoparticles), further accelerated by concentrated stresses originating from different volume changes along different directions of these nanoparticles, the processes somewhat analogous to a stress-induced corrosion [98,99]. The cathode performance can be significantly improved by defect engineering, such as introducing twin boundaries into spinel cathodes [100] or pumping surface defects into bulk lattice [101].

Recent studies showed that single-crystal cathode materials (with grain sizes significantly larger than those in polycrystalline microspheres) have a noticeably better stability. Single-crystalline cathodes are able to work at higher voltages and offer a longer cycle life compared to polycrystalline cathodes [30,102,103]. When comparing polycrystalline and single-crystalline NCM cathodes, the differences in the degree of particle cracking, active surface areas, and Li diffusion rates become clearly visible [104]. Single-crystalline NCM could avoid cracks after cycling, the observed cracking of secondary particles in polycrystalline NCM, which could result in liquid electrolyte infiltration in the active cathode materials, lowering the charge-transfer resistance and increasing the apparent diffusion coefficient [104]. However, single-crystal cathodes could still undergo capacity fading due to the spatially inhomogeneous Li concentrations in single-crystal cathodes during cycling and the nonuniform stress induced by the coexistence of two phases [105].

4.2. Particle Size and Distribution

To achieve optimal performance, it is essential to optimize the architectural parameters in electrode design, particularly particle size and distribution, which play a vital role in determining the solid-state diffusion length of Li ions, electrode surface area, and porosity [106–112]. In general, smaller particles have a shorter solid-state diffusion length, which can lead to a lower overpotential and faster C-rate operation. On the other hand, the larger surface area of smaller particles results in a higher proportion of passivation layers (e.g., CEI) which could cause capacity loss over time. In contrast, a larger size of particles results in a longer solid-state diffusion path, which is regarded as one of the primary limiting factors for LIBs based on thin electrodes [109,113], in spite of their higher tap density and higher volumetric energy.

Primary particles mainly affect the solid-state diffusion of Li ions while secondary particle size distribution (PSD) affect the attainable electrode density and the electrolyte diffusion through the electrodes [111,114]. The polydispersity index (PDI) and PSD are critical factors to electrode performance [96,110,115,116]. Avoiding too large and too small particles and attaining a medium-narrow PSD (with some smaller particles filling some of the voids between the larger ones, but not blocking such voids) enables better packing density and sufficiently fast improved electrolyte access, resulting in higher capacity and more consistent performance. In contrast, too broad PSD with excessively coarse particles could lower the attainable electrode smoothness and, thus, effective packing density, while a large portion of very small particles may block the pores and hinder electrolyte access, resulting in a lower capacity, poor rate, and less consistent performance. Primary particles are prone to heterogeneity in reaction kinetics due to variations in size and shape distribution, and secondary particles are more prone to cracking and detachment from the carbon/binder domain (CBD), leading to increased heterogeneity in the electrode microstructure [117–124]. Achieving a relatively uniform distribution of particles with controlled size is challenging and can result in heterogeneous reactions within the electrode. In practical electrode assemblies, active materials are embedded in the CBD, which can further complicate the charge distribution scenario [125,126]. CBD detachment and non-uniform voids distribution can induce a mismatch between ionic conductivity and electronic conductivity, compromising the effective utility of active particles. Heterogeneity at the CBD level can lead to a non-uniform percolated pore network and ionic transport resistance, which becomes worse after calendaring and can cause high current flux locally [119]. These issues can lead to reduced battery performance and durability.

A uniform size distribution and particle network and optimization of the space-controlled composition and porosity within the composite electrode (e.g., near a current collector vs. A separator) is expected to enhance electrochemical performance, reduce polarization, and result in better cycle stability [115,118,127,128]. Electrodes with vertically oriented particles or vertically oriented pores can improve rate performance without sacrificing gravimetric energy density [129–131]. The planar shape coupled with horizontal orientation and wide size distribution of active particles, on the other hand, not only may slow down Li-ion transport, but also result in a heterogeneous distribution of current and nonuniform lithiation between particles and along the through-thickness direction [132]. A mixture of small and large particles would be beneficial for attaining higher packing density and, thus, higher volumetric energy density in stationary energy storage. However, there are trade-offs to consider when optimizing particle size and distribution [133]. For instance, increasing either overall electrode density (by using particle size mixtures) or increasing areal capacity loading can generally degrade rate performance, but these could be counter-balanced by reducing electrode tortuosity, thus enhancing electrolyte wetting and minimizing effective through-electrode ion diffusion paths. Therefore, particle size, size distribution, particle shape, particle orientation within the electrode as well as the electrode pore size, pore orientation, and pore tortuosity must all be carefully considered during electrode design to ensure optimal performance.

4.3. Tortuosity

Tortuosity refers to the extent to which the path of the pore is convoluted and twisted, thus impeding the diffusion of ions within the electrode. Tortuosity is another important factor that impacts the ionic conductivity of an electrode, because the effective ionic conductivity (D_{eff}) is usually influenced by porosity (ϵ), tortuosity (τ), and intrinsic ion conductivity (D) of the electrolyte, that is $D_{\text{eff}} = D(\epsilon/\tau)$ [134]. A higher porosity can enhance the mass transport but leads to lower volumetric capacity and, additionally, could lead to a lower mechanical strength, electrode cracking, or delamination. In the electrode design, minimizing tortuosity is essential to improve ion transport in thick electrodes because effective ionic conductivity is inversely proportional to tortuosity [90,126,135,136]. The transmission line model analysis (TLM) is used to measure ionic resistance and determine McMullin number and tortuosity through electrochemical measurements [135]. Decreasing these values in dense and thick electrodes can decrease ion diffusion time, reduce overall impedance Z , and improve rate performance under high current densities. Low-tortuosity pore design is an effective approach to enhance ion transfer kinetics in thick electrodes. Achieving both fast ion and electron transport pathways is essential for optimal thick electrode design since thick electrodes with high areal capacity may cause mass transport limitations at elevated C-rates. However, there is a trade-off between porosity and tortuosity, and achieving a balance between the two is crucial for optimal battery performance.

4.4. Electrode Architecture

High-performance thick electrodes require the design of the overall architecture of cathode electrodes by considering the active material crystallinity, particle size, shape and surface area, the distribution, size, and shape of the conductive additives and the binder, and the resulting electrode porosity and tortuosity. For example, the difference in the porosity distribution in top and bottom layers of the electrode could affect the key electrode features such as physical, mechanical, chemical, and electrochemical properties. Pore engineering is a promising approach to improve the performance of battery electrodes by designing a microstructure with vertically oriented pore arrays [94,137]. Techniques such as high-temperature sintering, laser patterning, and density gradient electrodes were explored to create low-tortuosity pore structures that balance porosity and tortuosity [138–144]. However, manufacturing of thick or even ultra-thick electrodes (>100 μm) with (ultra)high mass loading is still difficult [91,145,146]. There are challenges to overcome, such as low volumetric capacity and lack of scalability in some of the explored approaches, and balancing ion transport and energy density, which can be affected by the potential decrease in energy density associated with high porosity. Therefore, careful control of porosity and tortuosity variation from the surface closer to separator to the contact closer to the current collector through electrode design and fabrication methods is crucial to facilitate ion transport, electrolyte infiltration, and ultimately improve battery performance [147,148]. In addition, heterogeneity can cause localized overcharging and Li plating, leading to rapid deterioration of the battery's microstructure and long-term performance. To address these issues, various techniques such as designing pore structures, using binder-free electrodes, attaining patterned electrodes, and 3D conductive skeletons could be further explored to help reduce heterogeneity, porosity, and tortuosity, thus improving battery performance and durability.

5. Conclusions

The development of next-generation LIBs calls for more considerations on cathode materials and electrode-processing technologies. In this review, we discussed the advances and challenges in current cathode materials, binders, and processing technologies. We compared conventional intercalation cathodes and conversion cathodes to demonstrate their current issues and future potentials. To meet the practical demands, it is desirable to design thicker cathode electrodes with high packing energy and fast charging/discharging rates. We discussed several key performance parameters from crystal/particle to electrode levels.

From a practical fabrication prospective, however, one should additionally consider the mechanics of cathode materials and fully formed electrodes with mechanical tests conducted, such as tensile, compression, bending, and nail-penetration (or blunt-rod) tests, which will be important for the evaluation of both high-yield mass production and the battery safety. Additionally, commutating methods such as finite element analysis (FEA) calculations and simulations, and/or machine learning/artificial intelligence (AI) should be also taken into consideration [149–151]. Further technology developments on both advanced cathode materials and cathode fabrication processes will be critical to promote the rapid development of battery industry.

Author Contributions: Conceptualization, W.F.; methodology, W.F., Y.W. and D.K.; writing—original draft preparation, W.F., Y.W., D.K., K.K. and F.W.; writing—review and editing, W.F. and G.Y.; visualization, W.F., Y.W. and D.K.; supervision, W.F. and G.Y.; project administration, G.Y.; funding acquisition, G.Y. All authors have read and agreed to the published version of the manuscript.

Funding: This research received no external funding.

Data Availability Statement: Not applicable.

Acknowledgments: The authors acknowledge the support from Georgia Institute of Technology.

Conflicts of Interest: The authors declare no conflict of interest.

References

1. Boudet, H.S. Public perceptions of and responses to new energy technologies. *Nat. Energy* **2019**, *4*, 446–455. [[CrossRef](#)]
2. Gielen, D.; Boshell, F.; Saygin, D.; Bazilian, M.D.; Wagner, N.; Gorini, R. The role of renewable energy in the global energy transformation. *Energy Strategy Rev.* **2019**, *24*, 38–50. [[CrossRef](#)]
3. Li, M.; Lu, J.; Chen, Z. Amine, 30 Years of Lithium-Ion Batteries. *Adv. Mater.* **2018**, *30*, 1800561. [[CrossRef](#)] [[PubMed](#)]
4. Choi, D.; Shamim, N.; Crawford, A.; Huang, Q.; Vartanian, C.K.; Viswanathan, V.V.; Paiss, M.D.; Alam, M.J.E.; Reed, D.M.; Sprenkle, V.L. Li-ion battery technology for grid application. *J. Power Sources* **2021**, *511*, 230419. [[CrossRef](#)]
5. Fu, W.; Turcheniuk, K.; Naumov, O.; Mysyk, R.; Wang, F.; Liu, M.; Kim, D.; Ren, X.; Magasinski, A.; Yu, M.; et al. Materials and technologies for multifunctional, flexible or integrated supercapacitors and batteries. *Mater. Today* **2021**, *48*, 176–197. [[CrossRef](#)]
6. Nykvist, B.; Nilsson, M. Rapidly falling costs of battery packs for electric vehicles. *Nat. Clim. Chang.* **2015**, *5*, 329–332. [[CrossRef](#)]
7. Frith, J.T.; Lacey, M.J.; Ulissi, U. A non-academic perspective on the future of lithium-based batteries. *Nat. Commun.* **2023**, *14*, 420. [[CrossRef](#)]
8. Turcheniuk, K.; Bondarev, D.; Amatucci, G.G.; Yushin, G. Battery materials for low-cost electric transportation. *Mater. Today* **2021**, *42*, 57–72. [[CrossRef](#)]
9. Nitta, N.; Wu, F.; Lee, J.T.; Yushin, G. Li-ion battery materials: Present and future. *Mater. Today* **2015**, *18*, 252–264. [[CrossRef](#)]
10. Wu, F.; Yushin, G. Conversion cathodes for rechargeable lithium and lithium-ion batteries. *Energy Environ. Sci.* **2017**, *10*, 435–459. [[CrossRef](#)]
11. Wang, L.; Wu, Z.; Zou, J.; Gao, P.; Niu, X.; Li, H.; Chen, L. Li-free Cathode Materials for High Energy Density Lithium Batteries. *Joule* **2019**, *3*, 2086–2102. [[CrossRef](#)]
12. Fu, W.; Kim, D.; Wang, F.; Yushin, G. Stabilizing cathodes and interphases for next-generation Li-ion batteries. *J. Power Sources* **2023**, *561*, 232738. [[CrossRef](#)]
13. Li, J.; Fleetwood, J.; Hawley, W.B.; Kays, W. From Materials to Cell: State-of-the-Art and Prospective Technologies for Lithium-Ion Battery Electrode Processing. *Chem. Rev.* **2022**, *122*, 903–956.
14. Kwade, A.; Haselrieder, W.; Leithoff, R.; Modlinger, A.; Dietrich, F.; Droeder, K. Current status and challenges for automotive battery production technologies. *Nat. Energy* **2018**, *3*, 290–300. [[CrossRef](#)]
15. Gonçalves, R.; Lanceros-Méndez, S.; Costa, C.M. Electrode fabrication process and its influence in lithium-ion battery performance: State of the art and future trends. *Electrochem. Commun.* **2022**, *135*, 107210. [[CrossRef](#)]
16. Kuang, Y.; Chen, C.; Kirsch, D.; Hu, L. Thick Electrode Batteries: Principles, Opportunities, and Challenges. *Adv. Energy Mater.* **2019**, *9*, 1901457. [[CrossRef](#)]
17. Arnot, D.J.; Mayilvahanan, K.S.; Hui, Z.; Takeuchi, K.J.; Marschilok, A.C.; Bock, D.C.; Wang, L.; West, A.C.; Takeuchi, E.S. Thick Electrode Design for Facile Electron and Ion Transport: Architectures, Advanced Characterization, and Modeling. *Accounts Mater. Res.* **2022**, *3*, 472–483. [[CrossRef](#)]
18. Liu, Y.; Zhu, Y.; Cui, Y. Challenges and opportunities towards fast-charging battery materials. *Nat. Energy* **2019**, *4*, 540–550. [[CrossRef](#)]
19. Julien, C.M.; Mauger, A.; Zaghbi, K.; Groult, H. Comparative Issues of Cathode Materials for Li-Ion Batteries. *Inorganics* **2014**, *2*, 132–154. [[CrossRef](#)]

20. Jung, S.C.; Han, Y.-K. Monoclinic sulfur cathode utilizing carbon for high-performance lithium–sulfur batteries. *J. Power Sources* **2016**, *325*, 495–500.
21. Yabuuchi, N.; Sugano, M.; Yamakawa, Y.; Nakai, I.; Sakamoto, K.; Muramatsu, H.; Komaba, S. Effect of heat-treatment process on FeF₃ nanocomposite electrodes for rechargeable Li batteries. *J. Mater. Chem.* **2011**, *21*, 10035–10041. [[CrossRef](#)]
22. Muralidharan, N.; Self, E.C.; Nanda, J.; Belharouak, I. Next-Generation Cobalt-Free Cathodes—A Prospective Solution to the Battery Industry’s Cobalt Problem. *Transit. Met. Oxides Electrochem. Energy Storage* **2022**, *12*, 33–53.
23. Olivetti, E.A.; Ceder, G.; Gaustad, G.G.; Fu, X. Lithium-Ion Battery Supply Chain Considerations: Analysis of Potential Bottlenecks in Critical Metals. *Joule* **2017**, *1*, 229–243. [[CrossRef](#)]
24. Ciez, R.E.; Whitacre, J.F. Examining different recycling processes for lithium-ion batteries. *Nat. Sustain.* **2019**, *2*, 148–156. [[CrossRef](#)]
25. Li, W.; Erickson, E.M.; Manthiram, A. High-nickel layered oxide cathodes for lithium-based automotive batteries. *Nat. Energy* **2020**, *5*, 26–34. [[CrossRef](#)]
26. Mohanty, D.; Li, J.; Nagpure, S.C.; Wood, D.L.; Daniel, C. Understanding the structure and structural degradation mechanisms in high-voltage, lithium-manganese-rich lithium-ion battery cathode oxides: A review of materials diagnostics. *MRS Energy Sustain.* **2015**, *2*, E15. [[CrossRef](#)]
27. Ling, J.; Karuppiah, C.; Krishnan, S.G.; Reddy, M.V.; Misnon, I.I.; Ab Rahim, M.H.; Yang, C.-C.; Jose, R. Phosphate Polyanion Materials as High-Voltage Lithium-Ion Battery Cathode: A Review. *Energy Fuels* **2021**, *35*, 10428–10450. [[CrossRef](#)]
28. Zhang, S.S. Problems and their origins of Ni-rich layered oxide cathode materials. *Energy Storage Mater.* **2020**, *24*, 247–254. [[CrossRef](#)]
29. Jiang, M.; Danilov, D.L.; Eichel, R.-A.; Notten, P.H.L. A Review of Degradation Mechanisms and Recent Achievements for Ni-Rich Cathode-Based Li-Ion Batteries. *Adv. Energy Mater.* **2021**, *11*, 2103005. [[CrossRef](#)]
30. Zhao, W.; Zou, L.; Zhang, L.; Fan, X.; Zhang, H.; Pagani, F.; Brack, E.; Seidl, L.; Ou, X.; Egorov, K.; et al. Assessing Long-Term Cycling Stability of Single-Crystal Versus Polycrystalline Nickel-Rich NCM in Pouch Cells with 6 mAh cm^{−2} Electrodes. *Small* **2022**, *18*, 2107357. [[CrossRef](#)]
31. Park, G.-T.; Namkoong, B.; Kim, S.-B.; Liu, J.; Yoon, C.S.; Sun, Y.-K. Introducing high-valence elements into cobalt-free layered cathodes for practical lithium-ion batteries. *Nat. Energy* **2022**, *7*, 946–954. [[CrossRef](#)]
32. Olbrich, L.F.; Xiao, A.W.; Pasta, M. Conversion-type fluoride cathodes: Current state of the art. *Curr. Opin. Electrochem.* **2021**, *30*, 100779. [[CrossRef](#)]
33. Xu, J.; Ma, J.; Fan, Q.; Guo, S.; Dou, S. Recent Progress in the Design of Advanced Cathode Materials and Battery Models for High-Performance Lithium-X (X = O₂, S, Se, Te, I₂, Br₂). *Batter. Adv. Mater.* **2017**, *29*, 1606454. [[CrossRef](#)] [[PubMed](#)]
34. Mikhaylik, Y.V.; Akridge, J.R. Polysulfide Shuttle Study in the Li/S Battery System. *J. Electrochem. Soc.* **2004**, *151*, A1969–A1976. [[CrossRef](#)]
35. Edström, K.; Gustafsson, T.; Thomas, J. The cathode–electrolyte interface in the Li-ion battery. *Electrochimica Acta* **2004**, *50*, 397–403.
36. Wu, H.; Chan, G.; Choi, J.W.; Yao, Y.; McDowell, M.T.; Lee, S.W.; Jackson, A.; Yang, Y.; Hu, L.; Cui, Y. Stable cycling of double-walled silicon nanotube battery anodes through solid-electrolyte interphase control. *Nature Nanotechnol.* **2012**, *7*, 310–315. [[CrossRef](#)]
37. An, S.J.; Li, J.; Daniel, C.; Mohanty, D.; Nagpure, S.; Wood, D.L. The state of understanding of the lithium-ion-battery graphite solid electrolyte interphase (SEI) and its relationship to formation cycling. *Carbon* **2016**, *105*, 52–76. [[CrossRef](#)]
38. Román-Ramírez, L.A.; Apachitei, G.; Faraji-Niri, M.; Lain, M.; Widanage, W.D.; Marco, J. Understanding the effect of coating-drying operating variables on electrode physical and electrochemical properties of lithium-ion batteries. *J. Power Sources* **2021**, *516*, 230689. [[CrossRef](#)]
39. Defraeye, T. Advanced computational modelling for drying processes—A review. *Appl. Energy* **2014**, *131*, 323–344. [[CrossRef](#)]
40. Westphal, B.G.; Kwade, A. Critical electrode properties and drying conditions causing component segregation in graphitic anodes for lithium-ion batteries. *J. Energy Storage* **2018**, *18*, 509–517. [[CrossRef](#)]
41. Zhang, Y.S.; Courtier, N.E.; Zhang, Z.; Liu, K.; Bailey, J.J.; Boyce, A.M.; Richardson, G.; Shearing, P.R.; Kendrick, E.; Brett, D.J.L. A Review of Lithium-Ion Battery Electrode Drying: Mechanisms and Metrology. *Adv. Energy Mater.* **2021**, *12*, 2102233. [[CrossRef](#)]
42. Susarla, N.; Ahmed, S.; Dees, D.W. Modeling and analysis of solvent removal during Li-ion battery electrode drying. *J. Power Sources* **2018**, *378*, 660–670. [[CrossRef](#)]
43. Stein, M.; Mistry, A.; Mukherjee, P.P. Mechanistic Understanding of the Role of Evaporation in Electrode Processing. *J. Electrochem. Soc.* **2017**, *164*, A1616–A1627. [[CrossRef](#)]
44. Shi, Y.; Zhou, X.; Yu, G. Material and Structural Design of Novel Binder Systems for High-Energy, High-Power Lithium-Ion Batteries. *Accounts Chem. Res.* **2017**, *50*, 2642–2652. [[CrossRef](#)] [[PubMed](#)]
45. Zhao, Y.; Liang, Z.; Kang, Y.; Zhou, Y.; Li, Y.; He, X.; Wang, L.; Mai, W.; Wang, X.; Zhou, G.; et al. Rational design of functional binder systems for high-energy lithium-based rechargeable batteries. *Energy Storage Mater.* **2021**, *35*, 353–377. [[CrossRef](#)]
46. Chou, S.-L.; Pan, Y.; Wang, J.-Z.; Liu, H.K.; Dou, S.X. Small things make a big difference: Binder effects on the performance of Li and Na batteries. *Phys. Chem. Chem. Phys.* **2014**, *16*, 20347–20359. [[CrossRef](#)]
47. Chen, H.; Ling, M.; Hencz, L.; Ling, H.Y.; Li, G.; Lin, Z.; Liu, G.; Zhang, S. Exploring Chemical, Mechanical, and Electrical Functionalities of Binders for Advanced Energy-Storage Devices. *Chem. Rev.* **2018**, *118*, 8936–8982. [[CrossRef](#)]

48. Kuang, Y.; Chen, C.; Pastel, G.; Li, Y.; Song, J.; Mi, R.; Kong, W.; Liu, B.; Jiang, Y.; Yang, K.; et al. Conductive Cellulose Nanofiber Enabled Thick Electrode for Compact and Flexible Energy Storage Devices. *Adv. Energy Mater.* **2018**, *8*, 1802398. [[CrossRef](#)]
49. Kovalenko, I.; Zdyrko, B.; Magasinski, A.; Hertzberg, B.; Milicev, Z.; Burtovyy, R.; Luzinov, I.; Yushin, G. A Major Constituent of Brown Algae for Use in High-Capacity Li-Ion Batteries. *Science* **2011**, *334*, 75–79. [[CrossRef](#)]
50. Pieczonka, N.P.W.; Borgel, V.; Ziv, B.; Leifer, N.; Dargel, V.; Aurbach, D.; Kim, J.-H.; Liu, Z.; Huang, X.; Krachkovskiy, S.A.; et al. Lithium Polyacrylate (LiPAA) as an Advanced Binder and a Passivating Agent for High-Voltage Li-Ion Batteries. *Adv. Energy Mater.* **2015**, *5*, 1501008. [[CrossRef](#)]
51. Le, A.V.; Wang, M.; Noelle, D.J.; Shi, Y.; Meng, Y.S.; Wu, D.; Fan, J.; Qiao, Y. Using high-HFP-content cathode binder for mitigation of heat generation of lithium-ion battery. *Int. J. Energy Res.* **2017**, *41*, 2430–2438. [[CrossRef](#)]
52. Mu, P.; Zhang, H.; Jiang, H.; Dong, T.; Zhang, S.; Wang, C.; Li, J.; Ma, Y.; Dong, S.; Cui, G. Bioinspired Antiaging Binder Additive Addressing the Challenge of Chemical Degradation of Electrolyte at Cathode/Electrolyte Interphase. *J. Am. Chem. Soc.* **2021**, *143*, 18041–18051. [[CrossRef](#)] [[PubMed](#)]
53. Maazi, S.; Navarchian, A.H.; Khosravi, M.; Chen, P. Effect of poly (vinylidene fluoride)/poly (vinyl acetate) blend composition as cathode binder on electrochemical performances of aqueous Li-ion battery. *Solid State Ionics* **2018**, *320*, 84–91. [[CrossRef](#)]
54. Liu, S.; Zhong, H.; Zhang, C.; Yan, X.; Zhao, X.; Zhang, L. Improving the processability and cycling stability of nano-LiFePO₄cathode by using PVDF/TX binary binder. *Compos. Interfaces* **2019**, *26*, 1013–1024. [[CrossRef](#)]
55. Ahn, J.; Im, H.-G.; Lee, Y.; Lee, D.; Jang, H.; Oh, Y.; Chung, K.; Park, T.; Um, M.-K.; Yi, J.W.; et al. A novel organosilicon-type binder for LiCoO₂ cathode in Li-ion batteries. *Energy Storage Mater.* **2022**, *49*, 58–66. [[CrossRef](#)]
56. Xu, J.; Chou, S.-L.; Gu, Q.-f.; Liu, H.-K.; Dou, S.-X. The effect of different binders on electrochemical properties of LiNi_{1/3}Mn_{1/3}Co_{1/3}O₂ cathode material in lithium ion batteries. *J. Power Sources* **2013**, *225*, 172–178. [[CrossRef](#)]
57. Hu, S.; Li, Y.; Yin, J.; Wang, H.; Yuan, X.; Li, Q. Effect of different binders on electrochemical properties of LiFePO₄/C cathode material in lithium ion batteries. *Chem. Eng. J.* **2014**, *237*, 497–502. [[CrossRef](#)]
58. Das, P.; Elizalde-Segovia, R.; Zayat, B.; Salamat, C.Z.; Pace, G.; Zhai, K.; Vincent, R.C.; Dunn, B.S.; Segalman, R.A.; Tolbert, S.H.; et al. Enhancing the Ionic Conductivity of Poly(3,4-propylenedioxythiophenes) with Oligoether Side Chains for Use as Conductive Cathode Binders in Lithium-Ion Batteries. *Chem. Mater.* **2022**, *34*, 2672–2686. [[CrossRef](#)]
59. Pham, H.Q.; Kim, G.; Jung, H.M.; Song, S.-W. Fluorinated Polyimide as a Novel High-Voltage Binder for High-Capacity Cathode of Lithium-Ion Batteries. *Adv. Funct. Mater.* **2018**, *28*, 1704690. [[CrossRef](#)]
60. Dong, T.; Zhang, H.; Ma, Y.; Zhang, J.; Du, X.; Lu, C.; Shangguan, X.; Li, J.; Zhang, M.; Yang, J.; et al. A well-designed water-soluble binder enlightening the 5 V-class LiNi_{0.5}Mn_{1.5}O₄ cathodes. *J. Mater. Chem. A* **2019**, *7*, 24594–24601. [[CrossRef](#)]
61. Ma, Y.; Chen, K.; Ma, J.; Xu, G.; Dong, S.; Chen, B.; Li, J.; Chen, Z.; Zhou, X.; Cui, G. A biomass based free radical scavenger binder endowing a compatible cathode interface for 5 V lithium-ion batteries. *Energy Environ. Sci.* **2019**, *12*, 273–280. [[CrossRef](#)]
62. Ryou, M.-H.; Hong, S.; Winter, M.; Lee, H.; Choi, J.W. Improved cycle lives of LiMn₂O₄ cathodes in lithium ion batteries by an alginate biopolymer from seaweed. *J. Mater. Chem. A* **2013**, *1*, 15224–15229. [[CrossRef](#)]
63. Brilloni, A.; Poli, F.; Spina, G.E.; Samorì, C.; Guidi, E.; Gualandi, C.; Maisuradze, M.; Giorgetti, M.; Soavi, F. Easy recovery of Li-ion cathode powders by the use of water-processable binders. *Electrochimica Acta* **2022**, *418*, 140376. [[CrossRef](#)]
64. Zhang, T.; Li, J.-T.; Liu, J.; Deng, Y.-P.; Wu, Z.-G.; Yin, Z.-W.; Guo, D.; Huang, L.; Sun, S.-G. Suppressing the voltage-fading of layered lithium-rich cathode materials via an aqueous binder for Li-ion batteries. *Chem. Commun.* **2016**, *52*, 4683–4686. [[CrossRef](#)] [[PubMed](#)]
65. Su, A.; Pang, Q.; Chen, X.; Dong, J.; Zhao, Y.; Lian, R.; Zhang, D.; Liu, B.; Chen, G.; Wei, Y. Lithium poly-acrylic acid as a fast Li⁺ transport media and a highly stable aqueous binder for Li₃V₂(PO₄)₃ cathode electrodes. *J. Mater. Chem. A* **2018**, *6*, 23357–23365. [[CrossRef](#)]
66. Xia, J.; Wang, Z.; Rodrig, N.D.; Nan, B.; Zhang, J.; Zhang, W.; Lucht, B.L.; Yang, C.; Wang, C. Super-Reversible CuF(2) Cathodes Enabled by Cu(2⁺)-Coordinated Alginate. *Adv. Mater.* **2022**, *34*, e2205229. [[CrossRef](#)]
67. Kim, S.; Cho, M.; Lee, Y. Multifunctional Chitosan-rGO Network Binder for Enhancing the Cycle Stability of Li-S Batteries. *Adv. Funct. Mater.* **2020**, *30*, 1907680. [[CrossRef](#)]
68. Du, Z.; Rollag, K.M.; Li, J.; An, S.J.; Wood, M.; Sheng, Y.; Mukherjee, P.P.; Daniel, C.; Wood, D.L. Enabling aqueous processing for crack-free thick electrodes. *J. Power Sources* **2017**, *354*, 200–206. [[CrossRef](#)]
69. Hawley, W.B.; Parejiya, A.; Bai, Y.; Meyer, H.M.; Wood, D.L.; Li, J. Lithium and transition metal dissolution due to aqueous processing in lithium-ion battery cathode active materials. *J. Power Sources* **2020**, *466*, 228315. [[CrossRef](#)]
70. Loeffler, N.; Kim, G.T.; Mueller, F.; Diemant, T.; Kim, J.K.; Behm, R.J.; Passerini, S. In Situ Coating of Li[Ni_{0.33} Mn_{0.33} Co_{0.33}]O₂ Particles to Enable Aqueous Electrode Processing. *ChemSusChem* **2016**, *9*, 1112–1117. [[CrossRef](#)]
71. Kuenzel, M.; Bresser, D.; Diemant, T.; Carvalho, D.V.; Kim, G.T.; Behm, R.J.; Passerini, S. Complementary Strategies Toward the Aqueous Processing of High-Voltage LiNi(0.5) Mn(1.5) O(4) Lithium-Ion Cathodes. *ChemSusChem* **2018**, *11*, 562–573. [[CrossRef](#)] [[PubMed](#)]
72. Sahore, R.; Wood, D.L.; Kukay, A.; Grady, K.M.; Li, J. Belharouak, Towards Understanding of Cracking during Drying of Thick Aqueous-Processed LiNi_{0.8}Mn_{0.1}Co_{0.1}O₂ Cathodes. *ACS Sustain. Chem. Eng.* **2020**, *8*, 3162–3169. [[CrossRef](#)]
73. Bresser, D.; Buchholz, D.; Moretti, A.; Varzi, A.; Passerini, S. Alternative binders for sustainable electrochemical energy storage—The transition to aqueous electrode processing and bio-derived polymers. *Energy Environ. Sci.* **2018**, *11*, 3096–3127. [[CrossRef](#)]

74. Lux, S.F.; Schappacher, F.; Balducci, A.; Passerini, S.; Winter, M. Low Cost, Environmentally Benign Binders for Lithium-Ion Batteries. *J. Electrochem. Soc.* **2010**, *157*, A320–A325. [[CrossRef](#)]
75. Komaba, S.; Shimomura, K.; Yabuuchi, N.; Ozeki, T.; Yui, H.; Konno, K. Study on Polymer Binders for High-Capacity SiO Negative Electrode of Li-Ion Batteries. *J. Phys. Chem. C* **2011**, *115*, 13487–13495. [[CrossRef](#)]
76. Bauer, W.; Çetinel, F.A.; Müller, M.; Kaufmann, U. Effects of pH control by acid addition at the aqueous processing of cathodes for lithium ion batteries. *Electrochim. Acta* **2019**, *317*, 112–119. [[CrossRef](#)]
77. Lu, Y.; Zhao, C.-Z.; Yuan, H.; Hu, J.-K.; Huang, J.-Q.; Zhang, Q. Dry electrode technology, the rising star in solid-state battery industrialization. *Matter* **2022**, *5*, 876–898. [[CrossRef](#)]
78. Liu, J.; Ludwig, B.; Liu, Y.; Zheng, Z.; Wang, F.; Tang, M.; Wang, J.; Wang, J.; Pan, H.; Wang, Y. Scalable Dry Printing Manufacturing to Enable Long-Life and High Energy Lithium-Ion Batteries. *Adv. Mater. Technol.* **2017**, *2*, 1700106. [[CrossRef](#)]
79. Ludwig, B.; Liu, J.; Chen, I.M.; Liu, Y.; Shou, W.; Wang, Y.; Pan, H. Understanding Interfacial-Energy-Driven Dry Powder Mixing for Solvent-Free Additive Manufacturing of Li-Ion Battery Electrodes. *Adv. Mater. Interfaces* **2017**, *4*, 1700570. [[CrossRef](#)]
80. Ludwig, B.; Zheng, Z.; Shou, W.; Wang, Y.; Pan, H. Solvent-Free Manufacturing of Electrodes for Lithium-ion Batteries. *Sci. Rep.* **2016**, *6*, 23150. [[CrossRef](#)]
81. De la Torre-Gamarra, C.; Sotomayor, M.E.; Sanchez, J.-Y.; Levenfeld, B.; Várez, A.; Laïk, B.; Pereira-Ramos, J.-P. High mass loading additive-free LiFePO₄ cathodes with 500 μm thickness for high areal capacity Li-ion batteries. *J. Power Sources* **2020**, *458*, 228033. [[CrossRef](#)]
82. Maurel, A.; Grugeon, S.; Fleutot, B.; Courty, M.; Prashantha, K.; Tortajada, H.; Armand, M.; Panier, S.; Dupont, L. Three-Dimensional Printing of a LiFePO₄/Graphite Battery Cell via Fused Deposition Modeling. *Sci. Rep.* **2019**, *9*, 18031. [[CrossRef](#)]
83. Sun, C.; Liu, J.; Gong, Y.; Wilkinson, D.P.; Zhang, J. Recent advances in all-solid-state rechargeable lithium batteries. *Nano Energy* **2017**, *33*, 363–386. [[CrossRef](#)]
84. Hippauf, F.; Schumm, B.; Doerfler, S.; Althues, H.; Fujiki, S.; Shiratsuchi, T.; Tsujimura, T.; Aihara, Y.; Kaskel, S. Overcoming binder limitations of sheet-type solid-state cathodes using a solvent-free dry-film approach. *Energy Storage Mater.* **2019**, *21*, 390–398. [[CrossRef](#)]
85. Jiang, T.; He, P.; Liang, Y.; Fan, L.-Z. All-dry synthesis of self-supporting thin Li₁₀GeP₂S₁₂ membrane and interface engineering for solid state lithium metal batteries. *Chem. Eng. J.* **2021**, *421*, 129965. [[CrossRef](#)]
86. Nakamura, H.; Kawaguchi, T.; Masuyama, T.; Sakuda, A.; Saito, T.; Kuratani, K.; Ohsaki, S.; Watano, S. Dry coating of active material particles with sulfide solid electrolytes for an all-solid-state lithium battery. *J. Power Sources* **2019**, *448*, 227579. [[CrossRef](#)]
87. Zheng, C.; Tang, S.; Wen, F.; Peng, J.; Yang, W.; Lv, Z.; Wu, Y.; Tang, W.; Gong, Z.; Yang, Y. Reinforced cathode-garnet interface for high-capacity all-solid-state batteries. *Mater. Futur.* **2022**, *1*, 045103. [[CrossRef](#)]
88. Patry, G.; Romagny, A.; Martinet, S.; Froelich, D. Cost modeling of lithium-ion battery cells for automotive applications. *Energy Sci. Eng.* **2015**, *3*, 71–82. [[CrossRef](#)]
89. Eshetu, G.G.; Zhang, H.; Judez, X.; Adenusi, H.; Armand, M.; Passerini, S.; Figgemeier, E. Production of high-energy Li-ion batteries comprising silicon-containing anodes and insertion-type cathodes. *Nat. Commun.* **2021**, *12*, 5459. [[CrossRef](#)]
90. Heubner, C.; Nikolowski, K.; Reuber, S.; Schneider, M.; Wolter, M.; Michaelis, A. Recent Insights into Rate Performance Limitations of Li-ion Batteries. *Batter. Supercaps* **2021**, *4*, 268–285. [[CrossRef](#)]
91. Bo, Z.; Cheng, X.; Yang, H.; Guo, X.; Yan, J.; Cen, K.; Han, Z.; Dai, L. Ultrathick MoS₂ Films with Exceptionally High Volumetric Capacitance. *Adv. Energy Mater.* **2022**, *12*, 2103394. [[CrossRef](#)]
92. Lu, X.; Daemi, S.R.; Bertei, A.; Kok, M.D.R.; O'Regan, K.B.; Rasha, L.; Park, J.; Hinds, G.; Kendrick, E.; Brett, D.J.L.; et al. Microstructural Evolution of Battery Electrodes During Calendering. *Joule* **2020**, *4*, 2746–2768. [[CrossRef](#)]
93. Meyer, C.; Bockholt, H.; Haselrieder, W.; Kwade, A. Characterization of the calendering process for compaction of electrodes for lithium-ion batteries. *J. Mater. Process. Technol.* **2017**, *249*, 172–178. [[CrossRef](#)]
94. Shodiev, A.; Chouchane, M.; Gaberscek, M.; Arcelus, O.; Xu, J.; Oularbi, H.; Yu, J.; Li, J.; Morcrette, M.; Franco, A.A. Deconvoluting the benefits of porosity distribution in layered electrodes on the electrochemical performance of Li-ion batteries. *Energy Storage Mater.* **2022**, *47*, 462–471. [[CrossRef](#)]
95. Boyce, A.M.; Lu, X.; Brett, D.J.; Shearing, P.R. Exploring the influence of porosity and thickness on lithium-ion battery electrodes using an image-based model. *J. Power Sources* **2022**, *542*, 231779. [[CrossRef](#)]
96. Bläubaum, L.; Röder, F.; Nowak, C.; Chan, H.S.; Kwade, A.; Krewer, U. Impact of Particle Size Distribution on Performance of Lithium-Ion Batteries. *Chemelectrochem* **2020**, *7*, 4755–4766. [[CrossRef](#)]
97. Qiu, B.; Zhang, M.; Wu, L.; Wang, J.; Xia, Y.; Qian, D.; Liu, H.; Hy, S.; Chen, Y.; An, K.; et al. Gas–solid interfacial modification of oxygen activity in layered oxide cathodes for lithium-ion batteries. *Nat. Commun.* **2016**, *7*, 12108. [[CrossRef](#)]
98. Sun, H.H.; Ryu, H.-H.; Kim, U.-H.; Weeks, J.A.; Heller, A.; Sun, Y.-K.; Mullins, C.B. Beyond Doping and Coating: Prospective Strategies for Stable High-Capacity Layered Ni-Rich Cathodes. *ACS Energy Lett.* **2020**, *5*, 1136–1146. [[CrossRef](#)]
99. Zhu, J.; Zeng, K.; Lu, L. Cycling effects on surface morphology, nanomechanical and interfacial reliability of LiMn₂O₄ cathode in thin film lithium ion batteries. *Electrochimica Acta* **2012**, *68*, 52–59. [[CrossRef](#)]
100. Wang, R.; Chen, X.; Huang, Z.; Yang, J.; Liu, F.; Chu, M.; Liu, T.; Wang, C.; Zhu, W.; Li, S.; et al. Twin boundary defect engineering improves lithium-ion diffusion for fast-charging spinel cathode materials. *Nat. Commun.* **2021**, *12*, 3085. [[CrossRef](#)]
101. Yan, P.; Zheng, J.; Tang, Z.-K.; Devaraj, A.; Chen, G.; Amine, K.; Zhang, J.-G.; Liu, L.-M.; Wang, C. Injection of oxygen vacancies in the bulk lattice of layered cathodes. *Nat. Nanotechnol.* **2019**, *14*, 602–608. [[CrossRef](#)] [[PubMed](#)]

102. Ni, L.; Zhang, S.; Di, A.; Deng, W.; Zou, G.; Hou, H.; Ji, X. Challenges and Strategies towards Single-Crystalline Ni-Rich Layered Cathodes. *Adv. Energy Mater.* **2022**, *12*, 2201510. [[CrossRef](#)]
103. Deng, X.; Zhang, R.; Zhou, K.; Gao, Z.; He, W.; Zhang, L.; Han, C.; Kang, F.; Li, B. A Comparative Investigation of Single Crystal and Polycrystalline Ni-Rich NCMs as Cathodes for Lithium-Ion Batteries. *Energy Environ. Mater.* **2022**, *ahead of print*. [[CrossRef](#)]
104. Trevisanello, E.; Ruess, R.; Conforto, G.; Richter, F.H.; Janek, J. Polycrystalline and Single Crystalline NCM Cathode Materials—Quantifying Particle Cracking, Active Surface Area, and Lithium Diffusion. *Adv. Energy Mater.* **2021**, *11*, 2003400. [[CrossRef](#)]
105. Ryu, H.-H.; Namkoong, B.; Kim, J.-H.; Belharouak, I.; Yoon, C.S.; Sun, Y.-K. Capacity Fading Mechanisms in Ni-Rich Single-Crystal NCM Cathodes. *ACS Energy Lett.* **2021**, *6*, 2726–2734. [[CrossRef](#)]
106. Jiang, Z.; Li, J.; Yang, Y.; Mu, L.; Wei, C.; Yu, X.; Pianetta, P.; Zhao, K.; Cloetens, P.; Lin, F.; et al. Machine-learning-revealed statistics of the particle-carbon/binder detachment in lithium-ion battery cathodes. *Nat. Commun.* **2020**, *11*, 2310. [[CrossRef](#)]
107. Lim, J.; Li, Y.; Alsem, D.H.; So, H.; Lee, S.C.; Bai, P.; Cogswell, D.A.; Liu, X.; Jin, N.; Yu, Y.-S.; et al. Origin and hysteresis of lithium compositional spatiodynamics within battery primary particles. *Science* **2016**, *353*, 566–571. [[CrossRef](#)]
108. Wood, M.; Li, J.; Du, Z.; Daniel, C.; Dunlop, A.R.; Polzin, B.J.; Jansen, A.N.; Krumdick, G.K.; Wood, D.L. Impact of secondary particle size and two-layer architectures on the high-rate performance of thick electrodes in lithium-ion battery pouch cells. *J. Power Sources* **2021**, *515*, 230429. [[CrossRef](#)]
109. Zhang, J.; Qiao, J.; Sun, K.; Wang, Z. Balancing particle properties for practical lithium-ion batteries. *Particuology* **2022**, *61*, 18–29. [[CrossRef](#)]
110. Röder, F.; Sonntag, S.; Schröder, D.; Krewer, U. Simulating the Impact of Particle Size Distribution on the Performance of Graphite Electrodes in Lithium-Ion Batteries. *Energy Technol.* **2016**, *4*, 1588–1597. [[CrossRef](#)]
111. Lu, X.; Zhang, X.; Tan, C.; Heenan, T.M.M.; Lagnoni, M.; O'Regan, K.; Daemi, S.; Bertei, A.; Jones, H.G.; Hinds, G.; et al. Multi-length scale microstructural design of lithium-ion battery electrodes for improved discharge rate performance. *Energy Environ. Sci.* **2021**, *14*, 5929–5946. [[CrossRef](#)]
112. Zan, G.; Qian, G.; Gul, S.; Li, J.; Matusik, K.; Wang, Y.; Lewis, S.; Yun, W.; Pianetta, P.; Vine, D.J.; et al. In situ visualization of multicomponents coevolution in a battery pouch cell. *Proc. Natl. Acad. Sci. USA* **2022**, *119*, e2203199119. [[CrossRef](#)] [[PubMed](#)]
113. Zeng, C.; Liang, J.; Cui, C.; Zhai, T.; Li, H. Dynamic Investigation of Battery Materials via Advanced Visualization: From Particle, Electrode to Cell Level. *Adv. Mater.* **2022**, *34*, 2200777. [[CrossRef](#)] [[PubMed](#)]
114. Park, G.-T.; Ryu, H.-H.; Noh, T.-C.; Kang, G.-C.; Sun, Y.-K. Microstructure-optimized concentration-gradient NCM cathode for long-life Li-ion batteries. *Mater. Today* **2021**, *52*, 9–18. [[CrossRef](#)]
115. Wu, S.; Yu, B.; Wu, Z.; Fang, S.; Shi, B.; Yang, J. Effect of particle size distribution on the electrochemical performance of micro-sized silicon-based negative materials. *RSC Adv.* **2018**, *8*, 8544–8551. [[CrossRef](#)] [[PubMed](#)]
116. Jeon, D.H. Enhancing electrode wettability in lithium-ion battery via particle-size ratio control. *Appl. Mater. Today* **2021**, *22*, 100976. [[CrossRef](#)]
117. Parmananda, M.; Norris, C.; Roberts, S.A.; Mukherjee, P.P. Probing the Role of Multi-scale Heterogeneity in Graphite Electrodes for Extreme Fast Charging. *ACS Appl. Mater. Interfaces* **2022**, *14*, 18335–18352. [[CrossRef](#)]
118. Li, J.; Sharma, N.; Jiang, Z.; Yang, Y.; Monaco, F.; Xu, Z.; Hou, D.; Ratner, D.; Pianetta, P.; Cloetens, P.; et al. Dynamics of particle network in composite battery cathodes. *Science* **2022**, *376*, 517–521. [[CrossRef](#)]
119. Nguyen, T.-T.; Villanova, J.; Su, Z.; Tucoulou, R.; Fleutot, B.; Delobel, B.; Delacourt, C.; Demortière, A. 3D Quantification of Microstructural Properties of LiNi_{0.5}Mn_{0.3}Co_{0.2}O₂ High-Energy Density Electrodes by X-ray Holographic Nano-Tomography. *Adv. Energy Mater.* **2021**, *11*, 2003529. [[CrossRef](#)]
120. Song, J.; Park, J.; Appiah, W.A.; Kim, S.-S.; Munakata, H.; Kanamura, K.; Ryou, M.-H.; Lee, Y.M. 3D electrochemical model for a Single Secondary Particle and its application for operando analysis. *Nano Energy* **2019**, *62*, 810–817. [[CrossRef](#)]
121. Sarawutanukul, S.; Tomon, C.; Phattharasupakun, N.; Duangdangchote, S.; Duriyasart, F.; Chiochan, P.; Sawangphruk, M. Optimization of the Electrode Properties for High-Performance Ni-Rich Li-Ion Batteries. *ACS Appl. Mater. Interfaces* **2021**, *13*, 30643–30652. [[CrossRef](#)]
122. Mayer, J.K.; Almar, L.; Asylbekov, E.; Haselrieder, W.; Kwade, A.; Weber, A.; Nirschl, H. Influence of the Carbon Black Dispersing Process on the Microstructure and Performance of Li-Ion Battery Cathodes. *Energy Technol.* **2019**, *8*, 1900161. [[CrossRef](#)]
123. Chauhan, A.; Asylbekov, E.; Kespe, S.; Nirschl, H. Influence of carbon binder domain on the performance of lithium-ion batteries: Impact of size and fractal dimension. *Electrochem. Sci. Adv.* **2022**, *3*, e2100151. [[CrossRef](#)]
124. Ngandjong, A.C.; Lombardo, T.; Primo, E.N.; Chouchane, M.; Shodiev, A.; Arcelus, O.; Franco, A.A. Investigating electrode calendaring and its impact on electrochemical performance by means of a new discrete element method model: Towards a digital twin of Li-Ion battery manufacturing. *J. Power Sources* **2021**, *485*, 229320. [[CrossRef](#)]
125. Song, K.; Li, W.; Chen, Z.; Wu, X.; Zhou, Q.; Snyder, K.; Zhang, L. An effective approach to improve electrochemical performance of thick electrodes. *Ionics* **2021**, *27*, 1261–1270. [[CrossRef](#)]
126. Ju, Z.; Zhang, X.; Wu, J.; King, S.T.; Chang, C.-C.; Yan, S.; Xue, Y.; Takeuchi, K.J.; Marschilok, A.C.; Wang, L.; et al. Tortuosity Engineering for Improved Charge Storage Kinetics in High-Areal-Capacity Battery Electrodes. *Nano Lett.* **2022**, *22*, 6700–6708. [[CrossRef](#)] [[PubMed](#)]
127. Ebner, M.; Chung, D.-W.; García, R.E.; Wood, V. Tortuosity Anisotropy in Lithium-Ion Battery Electrodes. *Adv. Energy Mater.* **2014**, *4*, 1301278. [[CrossRef](#)]

128. Kikukawa, H.; Honkura, K.; Koyama, M. Influence of inter-particle resistance between active materials on the discharge characteristics of the positive electrode of lithium ion batteries. *Electrochim. Acta* **2018**, *278*, 385–395. [[CrossRef](#)]
129. Xiong, R.; Zhang, Y.; Wang, Y.; Song, L.; Li, M.; Yang, H.; Huang, Z.; Li, D.; Zhou, H. Scalable Manufacture of High-Performance Battery Electrodes Enabled by a Template-Free Method. *Small Methods* **2021**, *5*, 2100280. [[CrossRef](#)]
130. Zhang, Q.; Sun, C.; Fan, L.; Zhang, N.; Sun, K. Iron fluoride vertical nanosheets array modified with graphene quantum dots as long-life cathode for lithium ion batteries. *Chem. Eng. J.* **2019**, *371*, 245–251. [[CrossRef](#)]
131. Zhang, X.; Hui, Z.; King, S.T.; Wu, J.; Ju, Z.; Takeuchi, K.J.; Marschilok, A.C.; West, A.C.; Takeuchi, E.S.; Wang, L.; et al. Gradient Architecture Design in Scalable Porous Battery Electrodes. *Nano Lett.* **2022**, *22*, 2521–2528. [[CrossRef](#)] [[PubMed](#)]
132. Lu, X.; Bertei, A.; Finegan, D.P.; Tan, C.; Daemi, S.R.; Weaving, J.S.; O'Regan, K.B.; Heenan, T.M.M.; Hinds, G.; Kendrick, E.; et al. 3D microstructure design of lithium-ion battery electrodes assisted by X-ray nano-computed tomography and modelling. *Nat. Commun.* **2020**, *11*, 2079. [[CrossRef](#)] [[PubMed](#)]
133. Zhu, P.; Slater, P.R.; Kendrick, E. Insights into architecture, design and manufacture of electrodes for lithium-ion batteries. *Mater. Des.* **2022**, *223*, 111208. [[CrossRef](#)]
134. Thorat, I.V.; Stephenson, D.E.; Zacharias, N.A.; Zaghbi, K.; Harb, J.N.; Wheeler, D.R. Quantifying tortuosity in porous Li-ion battery materials. *J. Power Sources* **2009**, *188*, 592–600. [[CrossRef](#)]
135. Landesfeind, J.; Hattendorff, J.; Ehrl, A.; Wall, W.A.; Gasteiger, H.A. Tortuosity Determination of Battery Electrodes and Separators by Impedance Spectroscopy. *J. Electrochem. Soc.* **2016**, *163*, A1373. [[CrossRef](#)]
136. Parikh, D.; Christensen, T.; Li, J. Correlating the influence of porosity, tortuosity, and mass loading on the energy density of LiNi_{0.6}Mn_{0.2}Co_{0.2}O₂ cathodes under extreme fast charging (XFC) conditions. *J. Power Sources* **2020**, *474*, 228601. [[CrossRef](#)]
137. Bae, C.-J.; Erdonmez, C.K.; Halloran, J.W.; Chiang, Y.-M. Design of Battery Electrodes with Dual-Scale Porosity to Minimize Tortuosity and Maximize Performance. *Adv. Mater.* **2013**, *25*, 1254–1258. [[CrossRef](#)]
138. Elango, R.; Nadeina, A.; Cadiou, F.; de Andrade, V.; Demortière, A.; Morcrette, M.; Seznec, V. Impact of electrode porosity architecture on electrochemical performances of 1 mm-thick LiFePO₄ binder-free Li-ion electrodes fabricated by Spark Plasma Sintering. *J. Power Sources* **2021**, *488*, 229402. [[CrossRef](#)]
139. Kim, Y.; Drews, A.; Chandrasekaran, R.; Miller, T.; Sakamoto, J. Improving Li-ion battery charge rate acceptance through highly ordered hierarchical electrode design. *Ionics* **2018**, *24*, 2935–2943. [[CrossRef](#)]
140. Huang, C.; Grant, P.S. Coral-like directional porosity lithium ion battery cathodes by ice templating. *J. Mater. Chem. A* **2018**, *6*, 14689–14699. [[CrossRef](#)]
141. Huang, C.; Dontigny, M.; Zaghbi, K.; Grant, P.S. Low-tortuosity and graded lithium ion battery cathodes by ice templating. *J. Mater. Chem. A* **2019**, *7*, 21421–21431. [[CrossRef](#)]
142. Hyun, G.; Cao, S.; Ham, Y.; Youn, D.-Y.; Kim, I.-D.; Chen, X.; Jeon, S. Three-Dimensional, Submicron Porous Electrode with a Density Gradient to Enhance Charge Carrier Transport. *ACS Nano* **2022**, *16*, 9762–9771. [[CrossRef](#)] [[PubMed](#)]
143. Zhang, X.; Hui, Z.; King, S.; Wang, L.; Ju, Z.; Wu, J.; Takeuchi, K.J.; Marschilok, A.C.; West, A.C.; Takeuchi, E.S.; et al. Tunable Porous Electrode Architectures for Enhanced Li-Ion Storage Kinetics in Thick Electrodes. *Nano Lett.* **2021**, *21*, 5896–5904. [[CrossRef](#)] [[PubMed](#)]
144. Yari, S.; Hamed, H.; D'haen, J.; Van Bael, M.K.; Renner, F.U.; Hardy, A.; Safari, M. Constructive versus Destructive Heterogeneity in Porous Electrodes of Lithium-Ion Batteries. *ACS Appl. Energy Mater.* **2020**, *3*, 11820–11829. [[CrossRef](#)]
145. Gao, H.; Wu, Q.; Hu, Y.; Zheng, J.P.; Amine, K.; Chen, Z. Revealing the Rate-Limiting Li-Ion Diffusion Pathway in Ultrathick Electrodes for Li-Ion Batteries. *J. Phys. Chem. Lett.* **2018**, *9*, 5100–5104. [[CrossRef](#)]
146. Park, J.; Jeon, C.; Kim, W.; Bong, S.-J.; Jeong, S.; Kim, H.-J. Challenges, laser processing and electrochemical characteristics on application of ultra-thick electrode for high-energy lithium-ion battery. *J. Power Sources* **2021**, *482*, 228948. [[CrossRef](#)]
147. Lu, L.-L.; Lu, Y.-Y.; Zhu, Z.-X.; Shao, J.-X.; Yao, H.-B.; Wang, S.; Zhang, T.-W.; Ni, Y.; Wang, X.-X.; Yu, S.-H. Extremely fast-charging lithium ion battery enabled by dual-gradient structure design. *Sci. Adv.* **2022**, *8*, eabm6624. [[CrossRef](#)]
148. Wu, J.; Ju, Z.; Zhang, X.; Xu, X.; Takeuchi, K.J.; Marschilok, A.C.; Takeuchi, E.S.; Yu, G. Low-Tortuosity Thick Electrodes with Active Materials Gradient Design for Enhanced Energy Storage. *ACS Nano* **2022**, *16*, 4805–4812. [[CrossRef](#)]
149. Ma, Y. Computer Simulation of Cathode Materials for Lithium Ion and Lithium Batteries: A Review. *Energy Environ. Mater.* **2018**, *1*, 148–173. [[CrossRef](#)]
150. Lv, C.; Zhou, X.; Zhong, L.; Yan, C.; Srinivasan, M.; Seh, Z.W.; Liu, C.; Pan, H.; Li, S.; Wen, Y.; et al. Machine Learning: An Advanced Platform for Materials Development and State Prediction in Lithium-Ion Batteries. *Adv. Mater.* **2022**, *34*, 2101474. [[CrossRef](#)]
151. Liu, K.; Wei, Z.; Zhang, C.; Shang, Y.; Teodorescu, R.; Han, Q.-L. Towards Long Lifetime Battery: AI-Based Manufacturing and Management. *IEEE/CAA J. Autom. Sin.* **2022**, *9*, 1139–1165. [[CrossRef](#)]

Disclaimer/Publisher's Note: The statements, opinions and data contained in all publications are solely those of the individual author(s) and contributor(s) and not of MDPI and/or the editor(s). MDPI and/or the editor(s) disclaim responsibility for any injury to people or property resulting from any ideas, methods, instructions or products referred to in the content.